

Spatial and temporal variability of methane emissions and environmental conditions in a hyper-eutrophic fishpond

Petr Znachor^{1,2}, Jiří Nedoma¹, Vojtech Kolar^{1,2}, Anna Matoušů¹

¹Biology Centre of Czech Academy of Sciences, v.v.i., Institute of Hydrobiology, Na Sádkách 7, České Budějovice, 37005, Czech Republic

²Faculty of Science, University of South Bohemia, Branišovská 1760, České Budějovice, 37005, Czech Republic

Correspondence to: Anna Matoušů (anna.matousu@gmail.com)

Abstract. Estimations of methane (CH₄) emissions are often based on point measurements using either flux chambers or a transfer coefficient method which may lead to strong underestimation of the total CH₄ fluxes. In order to demonstrate more precise measurements of the CH₄ fluxes from an aquaculture pond, using higher resolution sampling approach we examined the spatiotemporal variability of CH₄ concentration in the water, related fluxes (diffusive and ebullitive) and relevant environmental conditions (temperature, oxygen, chlorophyll-a) during three diurnal campaigns in a hyper-eutrophic fishpond. Our data show remarkable variance spanning several orders of magnitude while diffusive fluxes accounted for only a minor fraction of total CH₄ fluxes (4.1–18.5 %). Linear mixed-effects models identified water depth as the only significant predictor of CH₄ fluxes. Our findings necessitate complex sampling strategies involving temporal and spatial variability for reliable estimates of the role of fishponds in a global methane budget.

Keywords: aquaculture, emissions, fishpond, freshwater, heterogeneity, methane

25 **1 Introduction**

26 Freshwater aquaculture ponds (fishponds) represent man-made counterparts to natural shallow lakes (Scheffer,
27 2004) which are mainly used for fish production (mostly of common carp, *Cyprinus carpio* L.) and water retention
28 in the landscape. Fishponds serve also as secondary biotope for various organisms (Kolar et al., 2021), supporting
29 noteworthy animal and plant diversity (Pokorný and Hauser, 2002). However, most fishponds suffer from high
30 fish stock densities, excessive carbon and nutrient loading from supplemental fish feeding, sewage pollution, and
31 fertiliser runoffs from agricultural catchments or nutrient mobilisation from the anoxic sediment layers (Pechar,
32 2000). As a result, the trophic structure of plankton communities has shifted towards a reduction of large
33 zooplankton and massive development of phytoplankton, especially cyanobacterial blooms (Potužák et al., 2007),
34 limiting light penetration in the water column. Rapid changes in the intensity of biological processes such as
35 photosynthesis and respiration often result in pronounced daily or seasonal fluctuations in dissolved oxygen (Baxa
36 et al., 2021), signalling decreasing ecosystem stability. The extent of anoxia, accumulation of organic biomass,
37 and rapid heating of the shallow water during summer result in enhanced production of greenhouse gases (Grasset
38 et al., 2018, Zhang et al., 2021; Bartosiewicz et al., 2021).

39 Most concerning are CH₄ emissions as freshwater aquaculture systems release more than 6 Tg CH₄ yr⁻¹ (Yuan et
40 al., 2019). Methane can be emitted via several pathways: simple molecular diffusion, ebullition (in the form of
41 bubbles released from oversaturated sediments), plant-mediated flux (Bastviken et al., 2004), but also through so
42 far neglected pathways including aeration, emissions from dry/drying sediments, or dredged organic material
43 (Kosten et al., 2020). Among all, ebullition is considered the dominant pathway (van Bergen et al., 2019; Kosten
44 et al., 2020), which can contribute 50–96 % (Casper et al., 2000; Xiao et al., 2017; van Bergen et al., 2019; Yang
45 et al., 2020; Zhao et al., 2021) to the total CH₄ flux. Along with the second important pathway – molecular
46 diffusion, both exhibit high spatiotemporal variability due to various physical and biological factors acting on very
47 short time scales, for instance, temperature (van Bergen et al., 2019), nutrient loading (Zhang et al., 2021), CH₄
48 production rates (Zhou et al., 2019), CH₄ oxidation rates (Sanseverino et al., 2012), dissolved oxygen concentration
49 (Xiao et al., 2017), management regime (Yang et al., 2019), or the quality of organic matter in the sediment
50 (Schmiedeskamp et al., 2021). Recently, the potential involvement of phytoplankton in CH₄ production and
51 emissions has been suggested (Yan et al., 2019; Bižić et al., 2020; Bartosiewicz et al., 2021). The complex
52 interactions between physical and biological factors lead to a dynamic and ever-changing environment,
53 characterised by high spatial and temporal variability of methane fluxes in ponds.

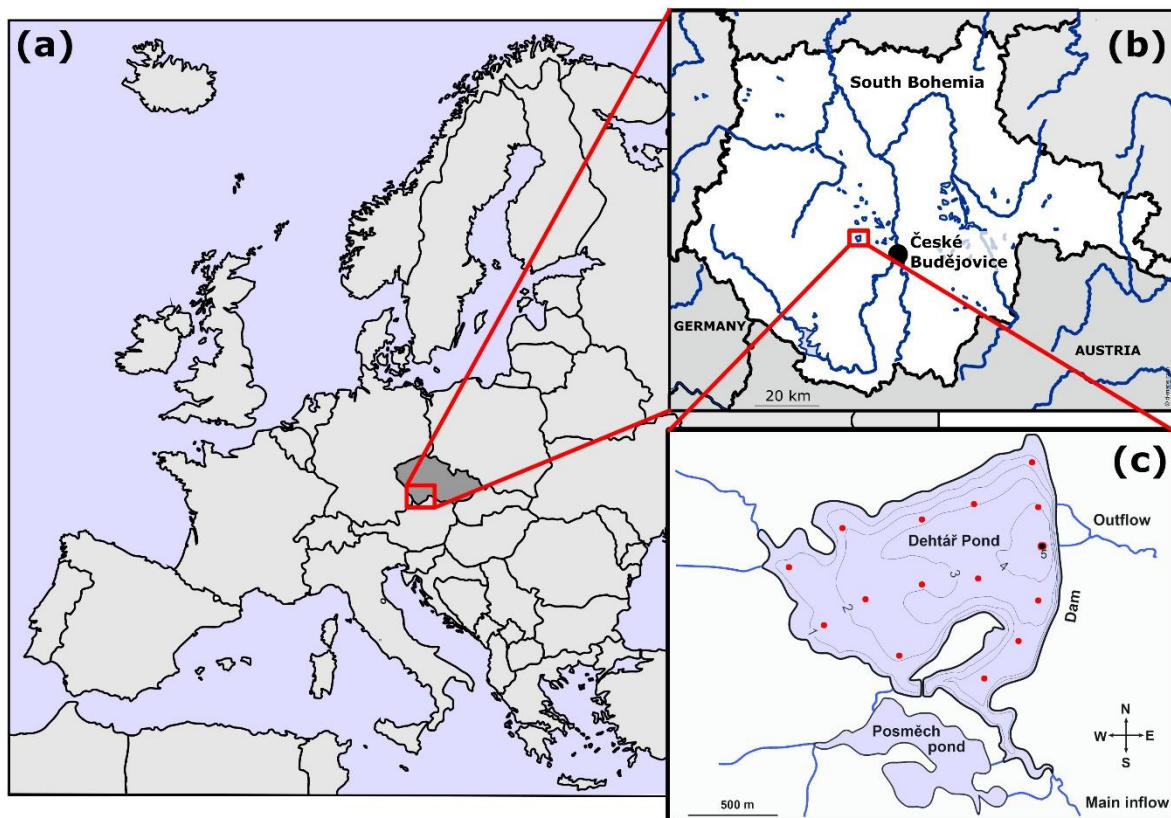
54 Although fishponds are recognised as powerful model systems for studies in ecology and evolutionary or
55 conservation biology (De Meester et al., 2005; Céréghino et al., 2008), the extent of environmental heterogeneity
56 in fishponds and shallow inland small waterbodies remains poorly understood (Ortiz and Wilkinson, 2021), largely
57 because the driving factors are either system-specific or highly variable on short time scales (Laas et al., 2012).
58 Most of current information on lentic ecosystem structure and function comes from single-site sampling, in which
59 measurements are taken over time at the deepest point in the lake, which does not sufficiently account for within-
60 lake spatial variation (Stanley et al., 2019). The motivation for our study was the growing concern about the role
61 of fishponds as important sources of CH₄ fluxes to the atmosphere (Wik et al., 2016). Unfortunately, the majority
62 of global CH₄ flux estimates rely on upscaling methods (DelSontro et al., 2018a) based on a limited number of
63 measurements that do not account for diurnal and seasonal variability or ecosystem spatial heterogeneity. Yang et
64 al. (2019) indicates that a larger number of spatial replicates over a number of months is mandatory to improve
65 the accuracy of whole-pond CH₄ flux estimates. The published research from other aquaculture studies have been
66 performed mainly in tropical and subtropical zones in fish or crab aquacultures (e.g. Hu et al., 2016; Ma et al.,
67 2018; Yang et al., 2019, 2020; Yuan et al., 2019, 2021). To better understand the spatial dynamics of CH₄ fluxes
68 and environmental heterogeneity in temperate freshwater shallow lake, we conducted a spatial sampling of the
69 hyper-eutrophic Dehtář fishpond (Czech Republic, Europe). Since the seasonal CH₄ production is strongly affected
70 by temperature, we focused on warm summer months where the total CH₄ fluxes were expected to be the highest
71 (Jansen et al., 2019). The objectives of our study were (i) to determine the spatial heterogeneity of CH₄ diffusive
72 and total fluxes and fundamental limnological variables (oxygen, temperature, chlorophyll-a) and their change
73 daily and monthly in the hyper-eutrophic pond, and (ii) to identify the factors that influence CH₄ fluxes to improve
74 our understanding of the importance of spatiotemporal variability for global estimates of CH₄ efflux to the
75 atmosphere.

76 **2 Material and Methods**

77 **2.1 Study site description**

78 The Dehtář fishpond (49°00'24.4"N 14°17'39.3"E) is a shallow man-made lake (average and maximum depth: 2.4
79 and 6 m) constructed in 1479 (Potužák et al., 2016). It is used for polycultural, semi-intensive production of
80 common carp, which account for 90–95 % of the fish biomass (Rutegwa et al., 2019). The pond is stocked with
81 two-year old carp harvested at the end of a two-year production cycle. To increase fish production, the original

82 management, based mainly on natural processes, has been intensified, and today manuring and supplementary
83 feeding in the form of grain or fish pellets, are common practices (Pechar, 2000). The pond lies in a flat agricultural
84 landscape at 406.4 m above sea level in the upper Vltava River basin in South Bohemia (Czech Republic) which
85 is characteristic with its network of fishponds (Fig. 1b). Due to the orography of the landscape, the Dehtář fishpond,
86 surrounded by narrow belts of littoral vegetation and adjacent to grassland and arable land, is exposed to wind,
87 mainly from the northwest (for aerial photograph, see Suppl. Fig 1). The catchment area is 91.4 km². The main
88 inflow is the Dehtářský stream in the south, while several smaller tributaries flow in from the west (Fig. 1c). The
89 fishpond has a dam 234 m long and 10 m high, with two outlets and a safety spillway. Covering 2.28 km², the
90 Dehtář fishpond is among the ten largest fishponds in the Czech Republic, holding a volume of 4.71×10^3 m³ and
91 having a water residence time of 146–445 days (Potužák et al., 2016).



92

93 **Figure 1.** Location (a, b; copyright www.d-maps.com; https://d-maps.com/carte.php?num_car=2232&lang=en and https://d-maps.com/carte.php?num_car=265046&lang=en; modified) and bathymetric map (c; credit Jiří Jarošík) of the sampled Dehtář
94 fishpond: blue lines indicate hydrological connections; red dots representing the sampling points. Highlighted sampling point
95 at the dam depicts the deepest site where vertical profiles were measured. Numbers indicate isobath depth.
96

97

98 2.2 Sampling design and measurement

99 To measure spatial heterogeneity and temporal changes in limnological parameters and methane fluxes, we
100 conducted three 36-hour surveys in summer 2019 (July 2–3, August 13–14, September 19–20). In the morning

101 (between 5–6 a.m.), we first measured surface values and vertical profiles of temperature, oxygen, and chlorophyll-
102 *a* concentration at the deepest point (see below for details). We subsequently installed 15 floating polyethylene
103 chambers (as shown in Fig. 1c), serving as fixed sampling sites and at the same time for accumulation of CH₄
104 fluxes (see further), starting in the western part of the fishpond. During installation (and further during each
105 sampling), temperature, pH, and oxygen concentration were measured at 0.3 m depth using the WTW 330i pH
106 meter and Oximeter (WTW, Weilheim, Germany). Vertical chlorophyll-*a* profiles were measured at each sampling
107 site using a submersible fluorescence probe (FluoroProbe, bbe Moldaenke, Kiel, Germany). From each site, the
108 average chlorophyll-*a* concentration in the surface layer (0–1 m depth) was used to assess the phytoplankton spatial
109 heterogeneity.

110 To minimise the chance that the differences observed among sites were due to time of day, we conducted repeated
111 measurements at the deepest point at the end of each sampling. This was relevant mainly to the initial measurement,
112 when the installation of all floating chambers took a total of 3 hours and 50 minutes. All other measurements, i.e.,
113 the interval between the first and last sampling point, required approximately two hours each. If there was a change,
114 all values were corrected for the sampling time by linear interpolation:

$$115 \quad P_{corr} = P_t + (P_{end} - P_0) \times \frac{(t-t_0)}{(t_{end}-t_0)} \quad (1)$$

116 where P_{corr} is the corrected value of a parameter, P_t is its value measured at the time t , P_0 and P_{end} are parameter
117 values measured at the deepest point at the start (time t_0) and at the end (t_{end}) of the sampling. In the evening and
118 morning of the second day (roughly at 12 h intervals), we performed additional measurements of spatial
119 heterogeneity, allowing us to assess diurnal and nocturnal changes. In addition, samples for measuring CH₄
120 concentration in the surface water were collected at each site and analysed as described below. To assess diurnal
121 variations in thermal structure and oxygen concentration in the water column, we made vertical profile
122 measurements at the deepest point (Fig. 1c) at 3–6 h intervals using the YSI EXO 2 multiparametric probe (YSI
123 Inc., Yellow Springs, USA).

124 **2.3 Methane measurements**

125 Water samples for determining CH₄ concentration in the surface water were collected at all 15 sampling sites in
126 triplicates into 20 ml glass bottles. The bottles were capped bubble-free under water with black butyl rubber
127 stoppers (Ochs, Germany) and sealed with aluminium crimps. Immediately after sampling, the water samples were
128 preserved by injecting 100 μ L of concentrated sulfuric acid to stop the microbial activity (Bussmann et al., 2015).
129 The samples were processed within one week in the laboratory using a headspace technique according to
130 McAuliffe (1971). Methane concentration in the headspace was measured using an HP 5890 Series II gas

131 chromatograph (Agilent Technologies, USA) and calculated with the solubility coefficient given by Yamamoto et
132 al. (1976).

133 Methane diffusive fluxes (F) were then calculated for each sampling site indirectly using the 2-layer model with
134 the equation:

$$135 \quad F = k(C_{sur} - C_{eq}) \quad (2)$$

136 where C_{sur} is the CH_4 concentration in surface water in $\mu\text{mol L}^{-1}$, C_{eq} is the CH_4 concentration in surface water in
137 equilibrium with the atmosphere in $\mu\text{mol L}^{-1}$, and k is the CH_4 exchange constant (cm h^{-1}). The atmospheric partial
138 pressure of CH_4 was set to 1.8 ppm. To compute k values, we first derived k_{600} estimates using a wind speed-based
139 relationship according to Crusius and Wanninkhof (2003):

$$140 \quad k_{600} = 1.68 + (0.228 \times U_{10}^{2.3}) \quad (3)$$

141 where U_{10} represents the wind speed at 10 m height (in m s^{-1} ; obtained from the nearby gauging station)
142 approximated by $U_{10} = 1.22U$, where U is the wind speed at 1.5 m height. We then converted k_{600} to k using the
143 eq. 4 according to Crusius and Wanninkhof (2003):

$$144 \quad k = k_{600} \left(\frac{Sc}{600} \right)^n \quad (4)$$

145 where k_{600} is the gas transfer velocity for a Schmidt number (Sc) of 600; n is a wind speed-dependent conversion
146 factor, for which we used $-2/3$ for $U_{10} < 3.7 \text{ m s}^{-1}$ (Jähne et al., 1987). The Schmidt number for CH_4 was calculated
147 according to Wanninkhof (2014):

$$148 \quad Sc = 1909.4 - 120.78t + 4.1555t^2 - 0.080578t^3 + 0.000658t^4 \quad (5)$$

149 where t ($^{\circ}\text{C}$) is the water temperature at the time of CH_4 extraction. The parameter C_{eq} in Eq. (1) was determined
150 from the equation:

$$151 \quad C_{eq} = \beta \times pCH_4 \quad (6)$$

152 where β is the solubility coefficient of CH_4 as a function of temperature according to Wiesenburg and Guinasso
153 (1979), and pCH_4 is the partial pressure of CH_4 in the atmosphere.

154 To estimate total CH_4 fluxes from the water column to the atmosphere (i.e., diffusive and ebullitive fluxes), we
155 measured CH_4 accumulation in open-bottom floating polyethylene chambers (volume 3.1 L; area 0.024 m^2). Each
156 gas chamber was anchored at individual 15 fixed sampling sites, but allowed to float freely on the water surface.
157 Gas was accumulating for approximately 12 h (each incubation had a start and end point) during particular
158 sampling period, i.e., during the day and night periods. Afterwards, 30 ml of gas was carefully taken from each
159 chamber, after mixing the headspace in the chamber, and stored in evacuated Exetainers[®] (Labco Limited, UK).
160 Chambers were ventilated after each sampling period to reset the incubation conditions. Methane fluxes were

161 calculated as the difference between initial background and final concentration in the chamber headspace and
162 expressed on the 1 m² area of the surface level per day according to Bastviken et al. (2004).

163 **2.4 Background limnological parameters**

164 During each campaign, water samples for analysis of nutrient concentration and phytoplankton composition were
165 collected from the surface at the deepest point using a Friedinger sampler. Water transparency was measured using
166 a Secchi disk. Total phosphorus (TP) and soluble reactive phosphorus (SRP) were analysed spectrophotometrically
167 according to Kopáček and Hejzlar (1993) and Murphy and Riley (1962), respectively. Concentrations of NH₄⁺ and
168 NO₃⁻ were determined according to the procedure of Kopáček and Procházková (1993) and Procházková (1959),
169 respectively. Phytoplankton samples were preserved with Lugol's solution and examined for species composition
170 with an inverted microscope (Olympus IMT-2). Weather data were obtained from the gauging station at the
171 fishpond dam.

172 **2.5 Statistical analyses**

173 Two-tailed paired Student's t-tests and Two-way ANOVA with post-hoc Tukey's multiple comparison test (Prism
174 9.3, GraphPad Software Inc., La Jolla, USA) tested for differences between diffusive and total CH₄ fluxes between
175 day and night and among three sampling campaigns, respectively. The percentage of data variability explained by
176 different factors (daytime, month and site) was calculated with the Two-way RM ANOVA. Contour graphs
177 illustrating changes in spatial heterogeneity of measured parameters were constructed in Surfer 10 (Golden
178 Software, Inc., Colorado, USA) using the kriging contouring method. Spatial heterogeneity was quantified for
179 each sampling by calculating the spatial variance (i.e. coefficient of variation of values measured at 15 sampling
180 sites; see, e.g. Fig 2):

$$181 \quad CV\% = 100 \times \frac{SD}{mean} \quad (7)$$

182 Higher spatial variance indicates increasing ecosystem patchiness. Linear mixed-effects models were used to
183 analyse the effects of O₂, pH, temperature, and water depth on the CH₄ diffusive fluxes with the random effect of
184 time of day nested within the effect of sampling date. The most parsimonious model was obtained by a manual
185 backward selection, where we sequentially removed all insignificant predictors (p > 0.05) using likelihood ratio
186 tests implemented in the drop1 function (Zuur et al., 2009). We also compared the slopes of the month-specific
187 regression lines produced by the model using analysis of covariance (Zar, 1984). Linear mixed-effects models
188 were implemented in the lme4 package version 1.1-21 (Bates et al., 2015), and Kenward-Roger F-tests were

189 computed using the ANOVA Type II function from the pbkrtest package version 0.4-7 (Halekoh and Hojsgaard,
 190 2014). The prediction of the resulting final model was visualised in the package ggeffects version 0.14.1 (Lüdtke,
 191 2018). Package performance version 0.4.4 (Lüdtke et al., 2020) was used to calculate Nakagawa's R^2 of the linear
 192 model. The statistical analyses were performed using R software (v. 3.5.2, R Core Team, 2018).

193 3 Results

194 3.1 Weather and background fishpond characteristics

195 Weather parameters varied among sampling campaigns. In July, clear skies prevailed with the daily air temperature
 196 above 30 °C (Table 1). During the August and September measurements, it was very cloudy, and daily air
 197 temperatures decreased to 22 and 18 °C, respectively. The water level was stable during the whole studied period
 198 with a monthly fluctuation of ~ 10 cm. Water transparency was low (15–40 cm), with an increasing trend towards
 199 the end of summer (Table 1). Concentrations of total phosphorus and soluble reactive phosphorus were high (Table
 200 1), consistent with a hyper-eutrophic state of the fishpond. In contrast, nitrogen concentrations were rather low,
 201 with ammonium nitrogen being the predominant form of inorganic N in the water (Table 1).

202 **Table 1:** Basic characteristics of the Dehtār fishpond during the studied period, measured at the surface at the deepest point.

	July	August	September
Weather	Clear sky, windy	Partly cloudy, no wind	Partly cloudy, no wind
Air temperature (°C)	25–32	20–22	11–18
Water temperature (°C)	24–29	22–23	16–17
Maximum wind speed (m s⁻¹)	3.2	0.8	0.9
PHAR (mol m⁻² day⁻¹)	9.5	3.4	5.0
Secchi depth (cm)	15	30	40
TP (µg L⁻¹)	568	527	406
SRP (µg L⁻¹)	100	200	107
N-NH₄⁺ (µg L⁻¹)	23	783	560
N-NO₃⁻ (µg L⁻¹)	14	23	46
Chl-<i>a</i> (µg L⁻¹)	456	156	185
Phytoplankton composition	Cyanobacteria	Cyanobacteria, green algae, cryptophytes	Cryptophytes, green algae

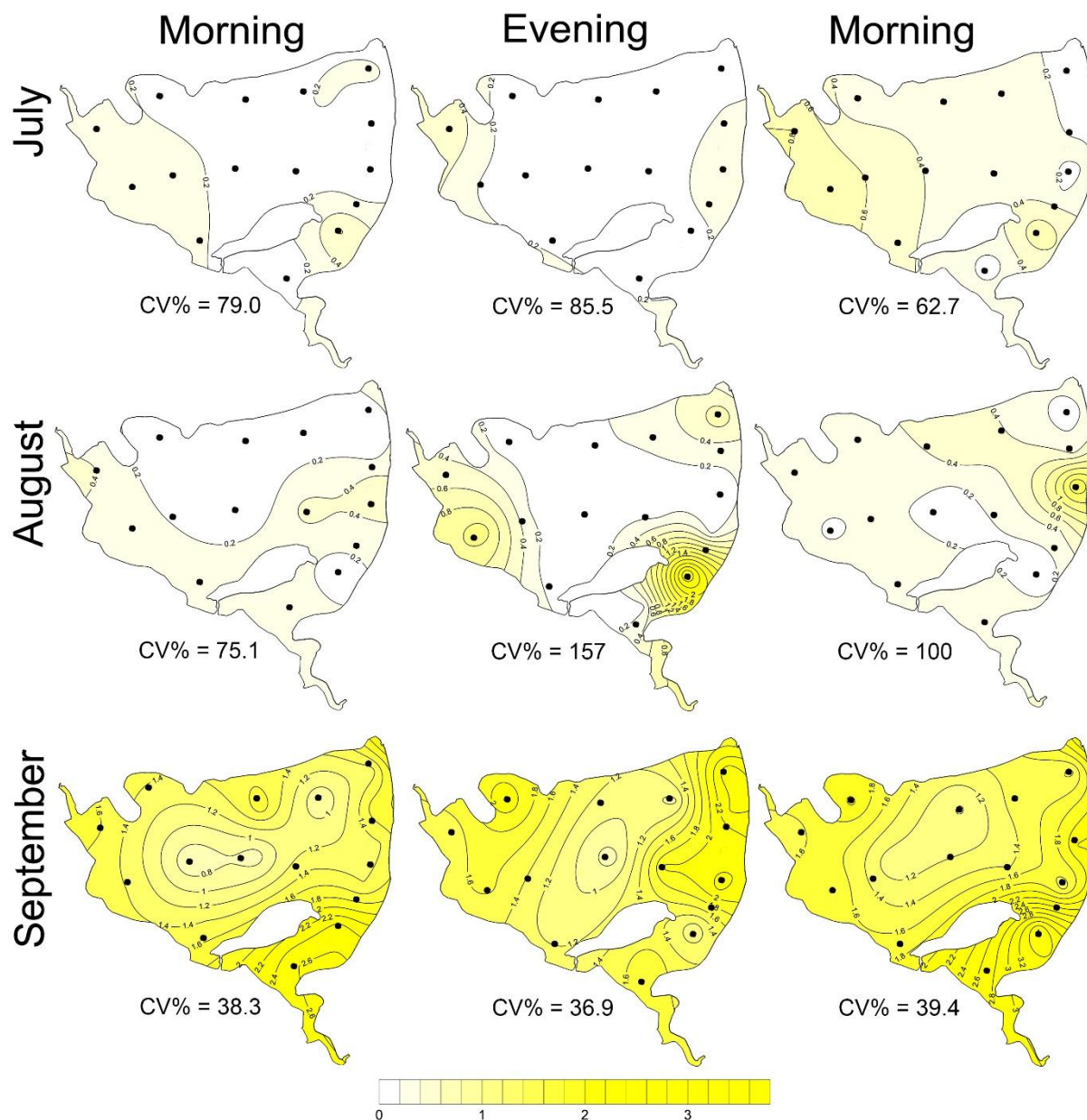
203

204 Chlorophyll-*a* concentrations were highest in July due to the dense cyanobacterial bloom accumulated at the
205 surface (Table 1). The phytoplankton consisted of only three cyanobacterial taxa: *Dolichospermum flos-aquae*,
206 *Planktothrix agardhii*, and *Raphidiopsis mediteranea*. In August, phytoplankton was more diverse but also
207 dominated by cyanobacteria: *P. agardhii*, *Aphanizomenon issatschenkoi*, and *D. flos-aquae*. In September,
208 cyanobacteria were absent and instead, cryptophytes (*Cryptomonas reflexa*), green algae (*Pediastrum*, *Coelastrum*
209 and *Desmodesmus*) and dinoflagellates (*Ceratium hirundinella*) prevailed.

210 **3.2 Methane concentration and fluxes**

211 The CH₄ concentration in surface water was highly supersaturated over the whole studied period. The obtained
212 values varied from 0.003 up to 3.75 μmol L⁻¹ (Fig. 2), which corresponded to saturation levels of 108–12 834%.
213 It is obvious, that the obtained data show remarkable variance: the mean (± SD) values were 0.22 ± 0.18 for July,
214 0.34 ± 0.45 for August, and 1.61 ± 0.61 μmol L⁻¹ for September (Suppl. Fig. 11).

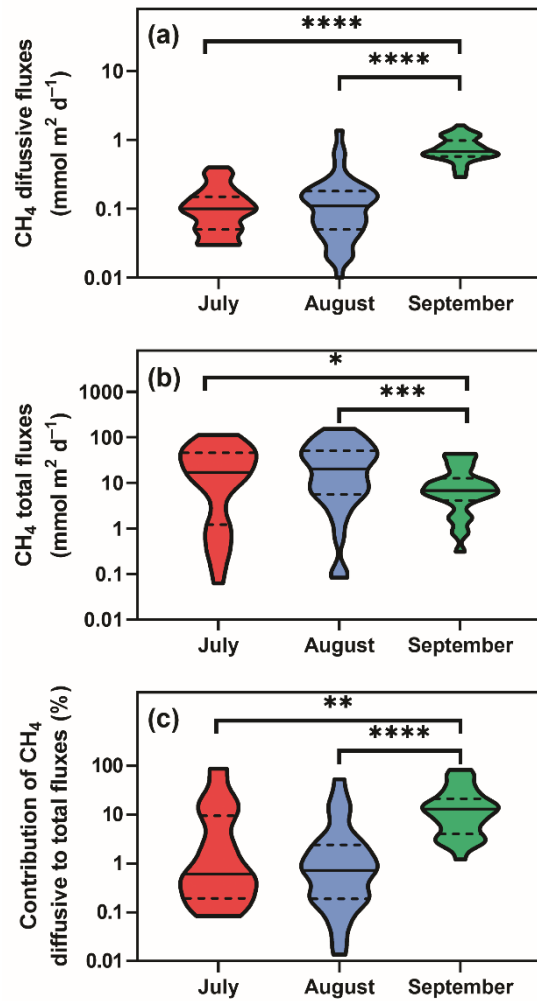
215



216

217 **Figure 2:** Surface methane concentrations ($\mu\text{mol L}^{-1}$). Contour graphs illustrating both seasonal and daily changes in spatial
 218 heterogeneity (indicated by the coefficient of variation, CV%) in the fishpond. Black dots representing the sampling sites.
 219

220 Diffusive fluxes (i.e., calculated from CH_4 concentration, see Eq. 2) showed the lowest values in July and August
 221 (average 0.12 and $0.16 \text{ mmol m}^{-2} \text{ d}^{-1}$, respectively) and pronouncedly peaked in September (average 0.78 mmol
 222 $\text{m}^{-2} \text{ d}^{-1}$, Fig. 3a). By contrast, in July and August, the average total CH_4 fluxes (obtained with floating chambers)
 223 showed the highest values (average $31.8 \text{ mmol m}^{-2} \text{ d}^{-1}$; ranging from 0.08 to $152 \text{ mmol m}^{-2} \text{ d}^{-1}$) while in
 224 September, total CH_4 fluxes were three times lower than before (average $11.8 \text{ mmol m}^{-2} \text{ d}^{-1}$, range 0.3 to 43.5
 225 $\text{mmol m}^{-2} \text{ d}^{-1}$, Fig 3b). As a result, diffusive fluxes accounted for only a minor fraction of total CH_4 fluxes to the
 226 atmosphere (on average, 9.2% in July, 4.1% in August, 18.5% in September, Fig. 3c).



227

228 **Figure 3:** Violin plots of CH₄ diffusive (a) and total fluxes (b) during the studied period. Panel (c) depicts differences in the
 229 percentage contribution of diffusive to total fluxes. Solid lines are medians, while dashed lines denote quartiles. Asterisks
 230 indicate significant differences (* p<0.05, ** p<0.01, *** p<0.001, **** p<0.0001) between sampling dates determined by
 231 two-way ANOVA with Tukey’s multiple comparison test. Note that a log scale is used here for clarity.

232

233 The total CH₄ fluxes show spatial variability within the fishpond that range four orders of magnitude (Fig. 3, 4;
 234 Suppl. Fig. 11; Suppl. Table 1). The observed spatial pattern showed high temporal variability on both daily and
 235 monthly scales (Fig. 2, 4, Suppl. Table 1). Most of the variability in CH₄ diffusive fluxes was explained by
 236 sampling date (62.4 %), while for the total CH₄ fluxes, spatial heterogeneity accounted for 87.2 % of data
 237 variability (Table 2). Using linear mixed-effects models, we identified water depth as the only significant predictor
 238 of total CH₄ fluxes (Df = 1, p < 0.0001, marginal Nakagawa’s R² = 0.348; Fig. 5).

239

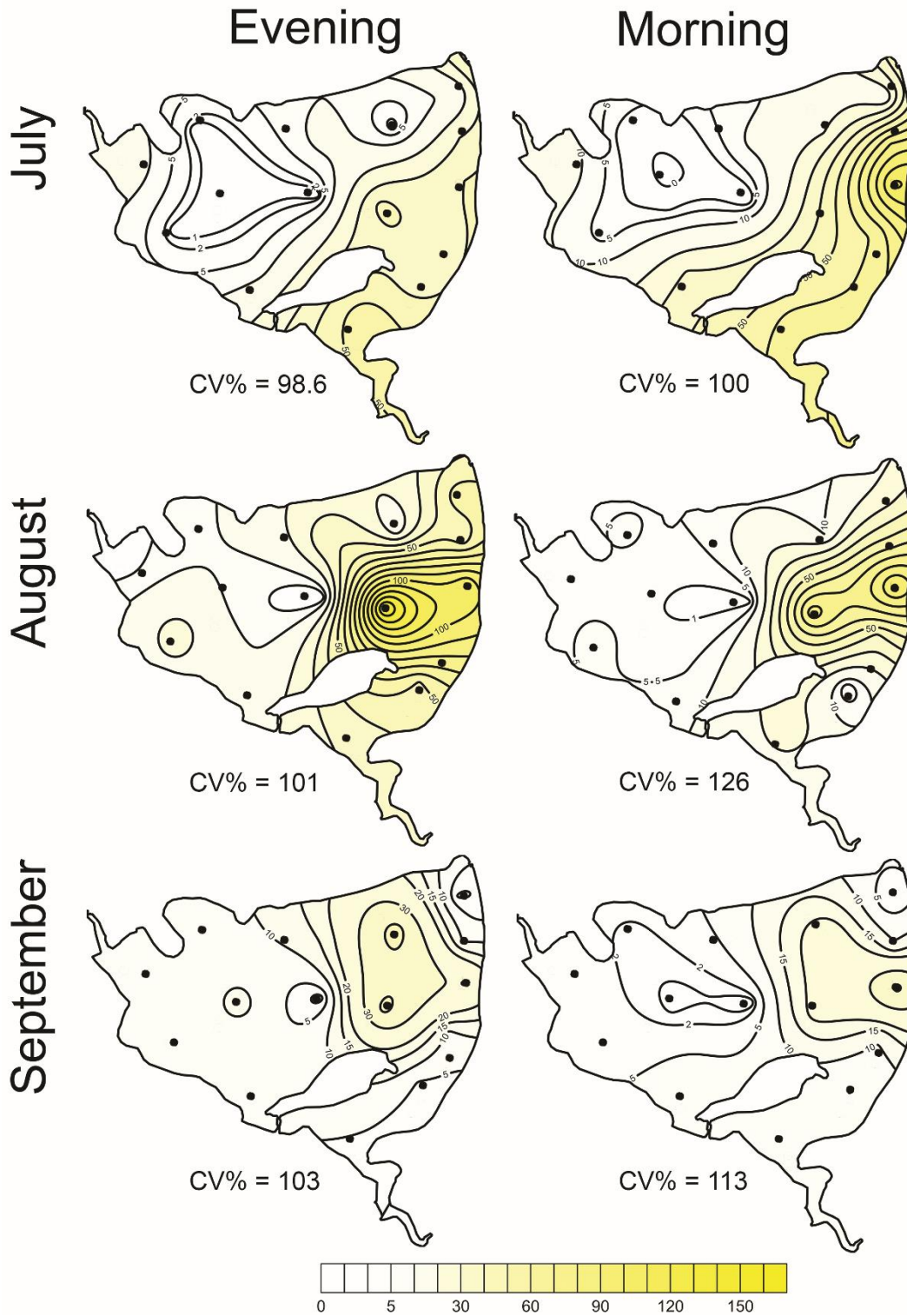
240

241

242 **Table 2:** The percentage of data variability explained by different factors (daytime, month = sampling date, and site)
 243 calculated with the Two-way RM ANOVA. Statistically significant values ($p < 0.01$) are bold.

	% of variability				Significance		
	Daytime	Month	Site	Unexplained	Daytime	Month	Site
CH₄ diffusive flux	2.3	62.4	13.2	22.1	0.0123	<0.0001	<i>n.s.</i>
CH₄ total flux	0.19	2.4	87.2	10.2	<i>n.s.</i>	<i>n.s.</i>	<0.0001
pH	4.4	64.9	11.1	19.6	0.0001	<0.0001	<i>n.s.</i>
Water temperature	3.3	92.3	2.5	1.9	<0.0001	<0.0001	<0.0001
O₂	21.7	48.1	13.8	16.4	<0.0001	<0.0001	0.0135
Chl-<i>a</i>	0.019	74.9	16.7	8.4	<i>n.s.</i>	<0.0001	<0.0001

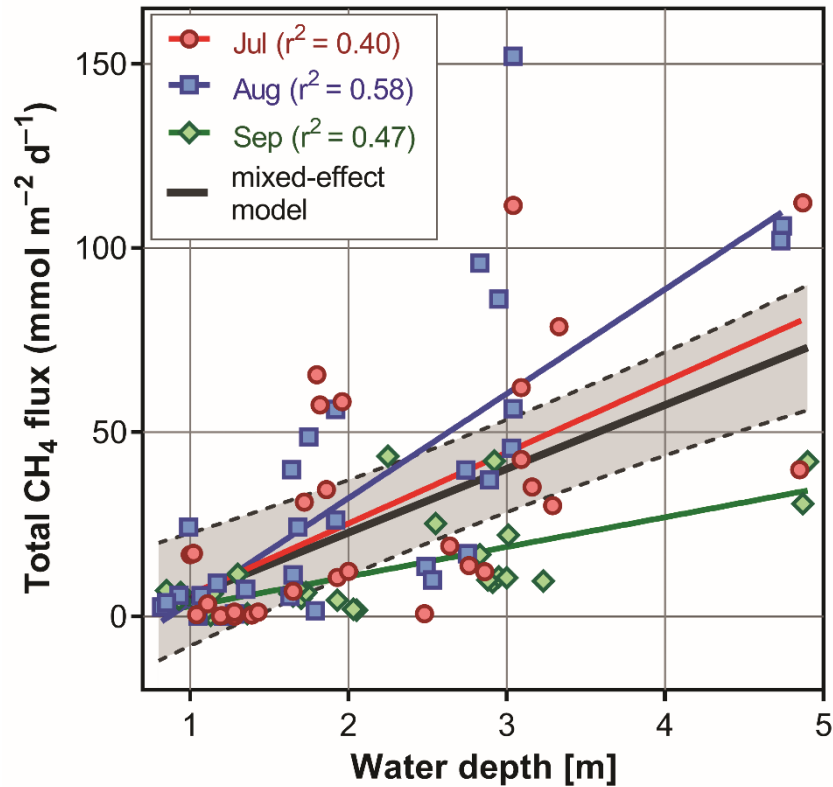
244 Interestingly, slopes of the linear regressions differed significantly among individual sampling campaigns (Fig. 5),
 245 indicating an additional season-related factor that affects CH₄ fluxes in the fishpond. Calculated CH₄ diffusive
 246 fluxes were not correlated with total fluxes. Linear mixed-effects models did not identify any significant predictor
 247 of the fluxes, indicating that factors and processes out of the study's scope are involved. We found no significant
 248 difference in either diffusive or total CH₄ fluxes between day and night.



249

250 **Figure 4:** Contour graphs of methane total fluxes in the Dehtář fishpond. Isopleths connect sites with the same value of
 251 methane fluxes ($\text{mmol m}^{-2} \text{ day}^{-1}$). CV% is a measure of spatial heterogeneity. Black dots representing the sampling sites.

252

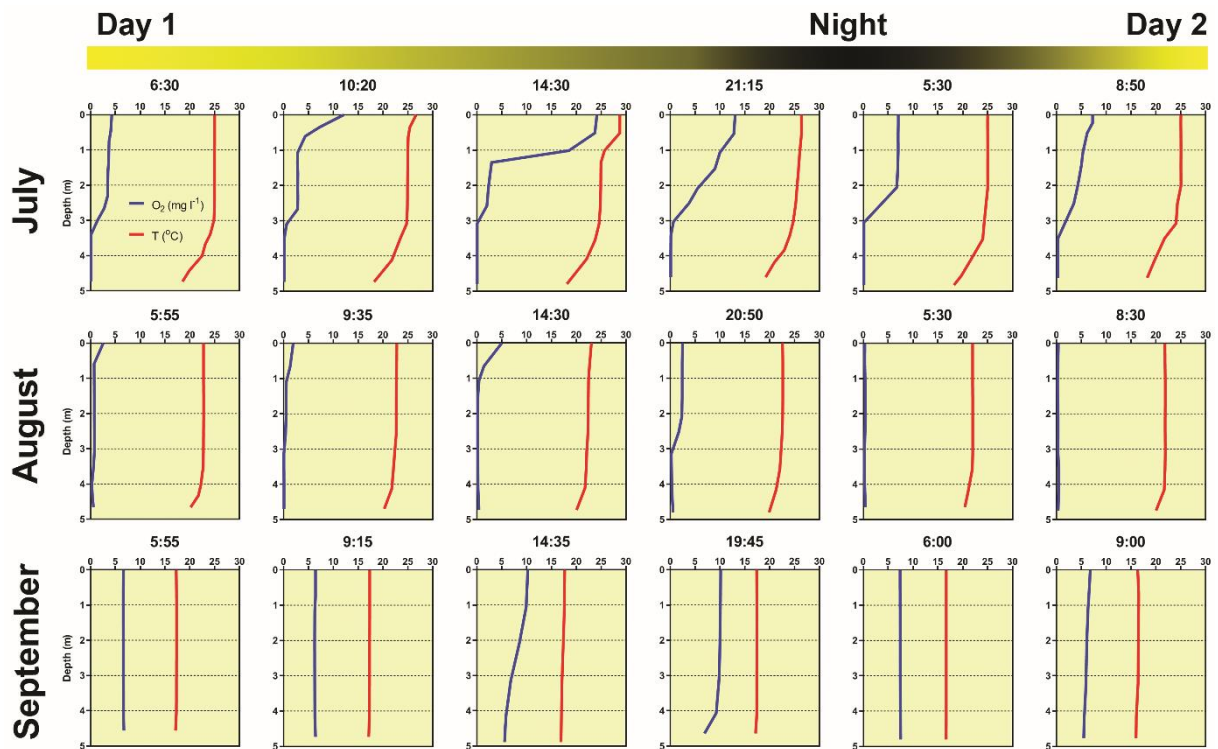


253

254 **Figure 5:** The most parsimonious linear mixed-effect model of methane total fluxes showing the water depth as the only
 255 significant predictor. Symbols are the measured values, the solid black line is the prediction, and dashed lines are 95th
 256 confidence intervals. Colours indicate month specific relation between total methane fluxes and water depth. Differences in
 257 slopes were tested using the F-test. In September, the slope of the regression line was significantly different from that in July
 258 and August.

259 3.3 Diurnal changes in vertical profiles of oxygen and temperature

260 Several contrasting patterns of vertical temperature and oxygen profiles occurred during summer 2019. Diurnal
 261 changes were most pronounced in July (Fig. 6). Surface temperatures varied from 25 °C in the morning to nearly
 262 30 °C in the afternoon. Thermal stratification of the water column was weak in the morning but became strongest
 263 at 14:30 with a thermocline at 0.5 m depth (Fig. 6). Later in the afternoon, the water column began to be mixed by
 264 wind. The morning vertical oxygen profile was characterised by a surface value of 4.3 mg L⁻¹, corresponding to
 265 51 % saturation and anoxia below 3 m.



266

267 **Figure 6:** Diurnal changes in vertical profiles of temperature and oxygen concentration measured at the deepest point of the
 268 fishpond. Numbers above each graph indicate the time of measurement.

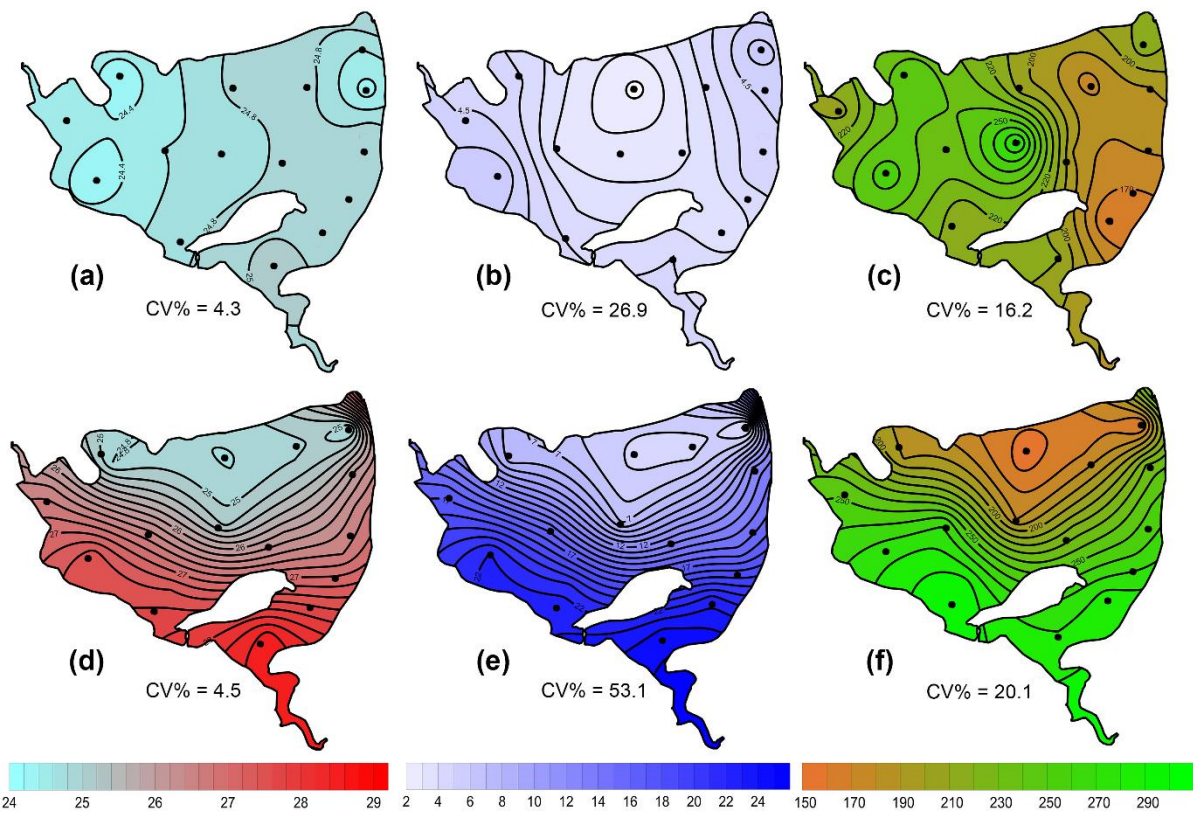
269 Due to the high photosynthetic activity of cyanobacteria, the surface oxygen concentration increased to 24 mg L^{-1}
 270 1 (320 % saturation, Fig. 6), and a steep oxycline was established at a depth of 0.5–1.5 m with no effect on the
 271 anoxic conditions at the deeper layers. Wind action eroded both the oxy- and thermoclines in the evening, and by
 272 the next morning, the vertical profiles were similar to those at the beginning.

273 In August, the water column was almost entirely mixed and low in oxygen in the morning, with only 2.6 mg L^{-1}
 274 (30 % saturation) of oxygen at the surface. Due to cloudy weather, the daily photosynthetic activity of
 275 phytoplankton resulted in only a slight increase in oxygen concentration at 0–1.5 m depth (4 mg L^{-1} , 47 %
 276 saturation). By the morning of the next day, the entire water column turned very close to anoxic (0.4 mg L^{-1} , 4 %
 277 saturation; Fig. 6), which in turn affected the spatial distribution of zooplankton, as evidenced by the formation of
 278 dense zooplankton clouds accumulated in the thin layer just at the surface (see Suppl. Fig. 3). In September, the
 279 water column was completely mixed, and we observed only weak daily changes in thermal and oxygen vertical
 280 structures (Fig. 6).

281 3.4 Effect of wind on spatial heterogeneity of temperature, oxygen and chlorophyll-*a*

282 During the summer, all measured parameters showed remarkable within-lake spatial heterogeneity (Suppl. Fig. 5–
 283 8). In July, meteorological conditions allowed for demonstrating the effect of wind on fishpond spatial

284 heterogeneity. In the morning, there were no substantial differences in the surface temperature and oxygen
 285 concentrations (Fig. 7ab). Phytoplankton biomass was accumulated mostly in the shallow western part, with the
 286 maximum in the centre (Fig. 7c). At 14:00, a light breeze started to blow from the northwest, achieving a maximum
 287 of 3.2 m s^{-1} (Suppl. Fig. 9). This episode lasted till the evening measurement, and the wind ceased by 21:00. The
 288 wind was strong enough to change spatial distribution substantially (Fig. 7d–f, Suppl. Fig. 4). In the evening, the
 289 surface water temperature on the windward (south) side of the fishpond was $\sim 4 \text{ }^\circ\text{C}$ higher than in the north (Fig.
 290 7d). The wind also induced order of magnitude differences in oxygen concentration along the north-south axis of
 291 the fishpond (3 mg L^{-1} of O_2 at the north, 24 mg L^{-1} of O_2 at the south; Fig. 7e) and affected phytoplankton
 292 distribution in the fishpond, resulting in remarkable bloom accumulation in the south (Fig. 7f, Suppl. Fig. 8).
 293 During the calm night after the disturbance, the north-south gradient substantially weakened. In August and
 294 September, the thermal heterogeneity of the pond was rather low, but the spatial distribution of oxygen and
 295 chlorophyll-*a* remained highly variable (Suppl. Fig. 5–8, Suppl. Table 1).



296
 297 **Figure 7:** Contour graphs of surface temperature (a, d; $^\circ\text{C}$), oxygen concentration (b, e; mg L^{-1}) and chlorophyll-*a*
 298 concentration (c, f; $\mu\text{g L}^{-1}$) measured on July 2 at different times of day: a, b and c are the morning measurements; d, e and f
 299 are evening measurements following a wind disturbance. Coefficient of variation (CV %) is a measure of spatial heterogeneity
 300 of measured parameters. Black dots representing the sampling sites.

301 **4 Discussion**

302 **4.1 Methane fluxes**

303 Assessing spatial heterogeneity of the CH₄ fluxes within a fishpond is critical for a reliable estimate of its
304 contribution to the global CH₄ budget. In our study, the variability in total CH₄ fluxes spanned several orders of
305 magnitude (ranging from 0.06 up to 1 121.3 mmol m⁻² d⁻¹), which is in agreement with similar studies (Casper et
306 al., 2000; DelSontro et al., 2016; Natchimuthu et al., 2016). However, most system-specific CH₄ flux estimates rely
307 on upscaling from a limited number of sites (Bastviken et al., 2004; Rasilo et al., 2015; Wik et al., 2016) because
308 obtaining spatial variability in CH₄ emission is methodologically challenging. In general, spatial heterogeneity
309 may reflect differences in water sources, physical mixing, local transformations and biogeochemical processes and
310 rates among lake habitats (Loken et al., 2019). In deep lakes, littoral areas can contribute disproportionately to
311 total lake CH₄ fluxes (Hofmann et al., 2010; Hofmann 2013, Natchimuthu et al., 2016; Schilder et al., 2013) and
312 are often missed by traditional sampling approaches (Wik et al., 2016). According to Wik et al. (2016), low
313 temporal and spatial resolutions are unlikely to cause overestimates. On the other hand, DelSontro et al. (2018b)
314 suggested that horizontal transport of CH₄ produced in littoral zones and the interaction between physical and
315 biological processes (e.g. air-water gas exchange, water column mixing, the interplay between CH₄ production
316 and microbial oxidation) may result in an underestimation of whole-lake CH₄ fluxes based on centre samples.
317 Similarly, Natchimuthu et al. (2016) found that up to 78 % underestimation would occur if samples obtained only
318 from the lake centre are used to extrapolate the total CH₄ flux. However, extrapolating our data from the deepest
319 point of the Dehtář fishpond would lead to an overestimation of the CH₄ fluxes by a factor of 2.9 (Suppl. Fig. 12).
320 The bias introduced by the deepest point measurement appears to be highly variable among systems with different
321 morphology, geographical location, mixing regimes or trophic states. For instance, analysis of 22 European lakes
322 during late summer has shown that spatially resolved CH₄ diffusive fluxes were highly variable for individual
323 lakes, yielding 55–300 % differences in the whole-lake estimates (Schilder et al., 2013). Schmiedeskamp et al.
324 (2021) observed an increase in CH₄ fluxes from the shore towards the centre in response to increasing sediment
325 C-content in two shallow German lakes. In line with these findings, our results provide further evidence that
326 spatially resolved data are needed to validate the uncertainties that come from using single-point samples to
327 represent whole-lake processes in hyper-eutrophic systems. As stated by Loken et al. (2019), rather than assuming
328 spatial homogeneity, scaling-up exercises of global carbon budgets should acknowledge the uncertainty that comes
329 from extrapolating from spatially limited data sets.

330 In the Dehtář fishpond, the total CH₄ fluxes increased with water depth, and this relationship was month specific.
331 The highest CH₄ fluxes at the deepest points may seem contradictory to previous studies, in which the highest
332 fluxes were typically observed in littoral areas (e.g., DelSontro et al., 2018b; Hofman et al., 2010; Natchimuthu et
333 al., 2016; Schilder et al., 2013). However, these findings are based on studying mostly large, shallow to medium-
334 deep oligotrophic lakes whose morphology, trophic state or oxygen regime sharply contrast with the hyper-
335 eutrophic Dehtář fishpond, where the upper two meters of the water column were oxygen-saturated while the
336 deepest strata were mostly anoxic, i.e., the extent and duration of bottom anoxia could be the most influential
337 factor contributing to the highest methane fluxes at the deepest point of the pond. In hyper-eutrophic systems, high
338 nutrient loading increases autochthonous primary production (Potužák et al., 2007; Rutegwa et al., 2019) and
339 promotes oxygen consumption and anaerobic decomposition in the sediments (Baxa et al., 2020), leading to
340 enhanced CH₄ production (Bastviken et al., 2004; Grasset et al., 2018). In aquaculture ponds in Southeast China,
341 CH₄ fluxes exhibited considerable spatial variations and peaked in the relatively deep feeding zone, where the
342 large loads of sediment organic matter fuelled CH₄ production (Yang et al., 2020). Furthermore, sediment
343 temperature was the strongest predictor of CH₄ fluxes in shallow ponds with anoxic hypolimnion (DelSontro et
344 al., 2016; Yang et al., 2020). It is, therefore, reasonable to assume that both temperature and oxygen concentration
345 in the sediment likely contributed to changes in observed CH₄ fluxes during the studied period in our study.
346 Although both parameters were not directly measured in the sediment, it can be deduced from their vertical profiles
347 that the probability of sediment anoxia was highest in August and lowest in September, and the sediment
348 temperature was lowest in September (see Fig. 5).

349 Our results agree with the generally accepted view that processes other than diffusive fluxes, most likely ebullition,
350 represent the major CH₄ pathway to the atmosphere in hyper-eutrophic ponds used for intensive fish production
351 (Kosten et al., 2020). Although freshwaters with high primary production are more likely to have high CH₄
352 ebullition rates (DelSontro et al., 2016), the dominant role of ebullition was also found across lentic systems
353 differing in size, trophic status or geographical location (Aben et al., 2017). Ebullition accounted on average for
354 56 % of total CH₄ fluxes in northern ponds in Canada (DelSontro et al., 2016), 49 and 71 % in two different zones
355 of Lake Taihu (Xiao et al., 2017) and 48-83 % in three Swedish lakes (Natchimuthu et al., 2016; Jansen et al.,
356 2019). The highest contribution was found in the small hyper-eutrophic Priest Pot (UK), where ebullition
357 represented 96 % of the total CH₄ flux from the pond (Casper et al., 2000). Apparently, the contribution of
358 ebullition can vary among systems and will remain uncertain until measurement designs cover enough
359 spatiotemporal variability to yield representative values for the whole ecosystem.

360 In shallow water bodies, a semi-stable flux of microbubbles was suggested to account for a significant portion of
361 the total CH₄ flux (Prairie and del Giorgio, 2013). When CH₄ concentration in the water column is above a certain
362 threshold of microbubble density, these microbubbles likely aggregate, fuse, and escape to the atmosphere from
363 buoyancy (Prairie and del Giorgio, 2013). Even a small fluctuation in hydrostatic pressure (e.g., due to changes in
364 atmospheric pressure) or lake water level was shown to trigger enhanced CH₄ ebullition (Bastviken et al., 2004;
365 Casper et al., 2000; Varadharajan and Hemond, 2012). Since ebullition rates increase exponentially with
366 temperature, CH₄ fluxes tend to peak in warm summer months (van Bergen et al., 2019). In our study, 1 % lower
367 air pressure in July and August than in September, along with bottom anoxia and higher water temperature, could
368 account for the enhanced release of CH₄ bubbles from the sediment (31.7 mmol m⁻² d⁻¹, >90 % of total CH₄ fluxes;
369 Suppl. Fig. 2). In September, when we observed the lowest water temperatures from the studied period and the
370 oxygen profile was rather uniform, ebullition accounted for 81 % (11 mmol m⁻² d⁻¹) of the total CH₄ fluxes. The
371 spatially pooled data of the total CH₄ fluxes measured in the Dehtář fishpond varied from 11.8 to 34.5 mmol m⁻²
372 d⁻¹, which is comparable with similar systems elsewhere (e.g., Bastviken et al., 2010; van Bergen et al., 2019;
373 Baron et al., 2022). To sum up, both diffusive fluxes and ebullition must be addressed to understand the magnitude
374 of total aquatic CH₄ fluxes and how their relative contributions vary across and within aquatic systems (Kosten et
375 al., 2020). Moreover, with an improved determination of CH₄ hot-spots and its causes, the management of ponds
376 could be changed accordingly and so the overall emissions reduced for example by decreasing P-availability and
377 dredging (Nijman et al., 2022).

378 **4.2 Effect of wind event on ecosystem spatial structure**

379 Sudden changes in ecosystem spatial structure in response to meteorological forcing have rarely been documented
380 (Loken et al., 2019) since they are hard to predict. Research into them using traditional methods requires intensive
381 effort or expensive instrumentation (Ortiz and Wilkinson, 2021), and it remains a matter of luck to obtain a relevant
382 dataset. In the July sampling campaign, we observed a strong impact of the wind on environmental heterogeneity
383 in the fishpond, which was apparent at a sub-daily time scale. Due to the methodological constraints, i.e., lack of
384 initial measurement, we can only speculate about the effect of wind on the total CH₄ fluxes. The northwest wind
385 during the day advected warmed surface water with cyanobacterial bloom from the north basin to the south. In the
386 evening, it resulted in bloom accumulation on the upward side and a north-south gradient of more than 4 °C and
387 20 mg L⁻¹ oxygen. After the winds fell off, the observed gradients declined during cooling at night. We assume
388 that the wind blowing across the pond surface drove buoyant cyanobacteria and surface water downwind and
389 caused an upwelling of deeper, colder, and hypoxic water on the upwind side. This wind-related circulation pattern

390 has been described as a “conveyer belt” in classical textbooks (Reynolds et al., 2006), held responsible for a
391 disruption of the thermal structure of the water column and the non-uniform spatial distribution of pH, oxygen,
392 CO₂ or CH₄ and also plankton assemblages (e.g., Loken et al., 2019; Natchimuthu et al., 2016; Rinke et al., 2009;
393 Ortiz and Wilkinson, 2021).

394 Similar to our study, mild winds (~4 m s⁻¹) were strong enough to redistribute heat and induce lake-wide
395 circulations driving upwelling and downwelling in 24 m deep Lake Pleasant (Czikowsky et al., 2018). As the wind
396 blows harder and lasts longer, the effects on ecosystem functioning may target higher trophic levels and become
397 more complex (Rinke et al., 2009). In Lake Constance, a three-day storm event with wind velocities of ~10 m s⁻¹
398 resulted in a lake-wide displacement of water masses and the formation of the 6–15 °C horizontal surface water
399 gradient, which in turn changed the spatial distribution of phytoplankton, zooplankton and juvenile fish (Rinke et
400 al., 2009). After several stormy days (wind velocities of 12–15 m s⁻¹), Čech et al. (2011) observed negative effects
401 of wind-driven changes in water temperature and wave action on perch (*Perca fluviatilis*) spawning in the Lake
402 Milada. Although wind events affect shallow and deep lakes differently, there is growing evidence that they can
403 have far-reaching consequences on the functioning of aquatic ecosystems by disrupting energy flows, nutrient
404 fluxes, productivity and reproduction, and consequently altering community composition and trophic interactions
405 in the short and long term (Stockwell et al., 2020). As the frequency, intensity, spatial extent and duration of these
406 extreme meteorological events are projected to increase due to ongoing climate change (Comou and Rahmstorf,
407 2012), there is an urgent need to better understand the mechanisms underlying their impacts on the maintenance
408 of the ecosystem services.

409 **4.3 Summer changes in the oxygen regime**

410 Our data demonstrate that shallow, hyper-eutrophic ponds have disrupted oxygen regimes (Baxa et al., 2021) with
411 anoxic hypolimnion and may experience severe whole-water column hypoxia critical for aquatic biota (Miranda
412 et al., 2001). The hypoxic periods may result, for example, from sudden weather change (Jeppesen et al., 1990)
413 and last several days, during which physical processes and phytoplankton photosynthesis cannot compensate for
414 intense community respiration (Baxa et al., 2021). This became obvious in August when severe oxygen depletion
415 was measured at the surface across the whole pond, mostly far below a critical level of 4.5 mg L⁻¹, when adverse
416 effects came into play (Banerjee et al., 2019). However, oxygen surface concentrations in shallow parts of the
417 pond were substantially higher regardless of the time of day, which contrasts with findings of Miranda et al. (2001),
418 who emphasised shallow waters as the most sensitive parts of lakes, where hypoxic events can occur due to the
419 respiration of sediment biota. The observed spatial gradients of oxygen may create temporal refugia which allow

420 fish to survive harsh conditions that occur in the deepest part of the pond. To minimise economic losses and
421 negative impacts on the ecosystem, future research should identify the interplay between meteorological forcing,
422 trophic status and anthropogenic pressures (e.g., management practices) that affect oxygen fluctuations at various
423 time scales.

424 **4.4 Study limitations**

425 Like in other research, there are some limitations in the current study. Since our measurement had only a limited
426 temporal resolution (three samplings during the summer season), it is not appropriate to extrapolate CH₄ emissions
427 for annual values. Noticeably, future research must increase the frequency of the sampling and include also
428 innovative techniques to measure CH₄ fluxes at multiple fishponds, with different management regime. In our
429 study, the 12-h deployment time of the floating chambers could have led to extensive gas accumulation, which in
430 turn might have resulted in an underestimation of the total CH₄ fluxes due to the dissolution of the CH₄ from the
431 chamber into the water once the equilibrium concentration in the chamber is overcome (Bastviken et al., 2010).
432 However, CH₄ concentrations in water corresponded to a supersaturation of several orders of magnitude, so the
433 introduced bias appears to be of minor importance. In any case, our daily spatially pooled total CH₄ fluxes (11.8–
434 34.5 mmol m⁻² d⁻¹) represent a rather conservative estimate for the global methane budget. In our study, we also
435 did not address the important processes that could shed light on the lake CH₄ budget, such as CH₄ oxidation rates
436 (Bastviken et al., 2008) or biological interaction (e.g., protistan grazing on CH₄ oxidising bacteria) in aquatic food
437 webs (Sanseverino et al., 2012) that can affect the overall CH₄ fluxes. We also lack information about spatial
438 differences in sediment microbiota and organic carbon content and compositions, which were found to affect CH₄
439 production rates (Berberich et al., 2020; Emerson et al., 2021). Despite the limitation mentioned above, our results
440 show that complementary spatial surveys help contextualise the fixed station dynamics and provide additional,
441 management-relevant information about the fishpond.

442 For improved monitoring strategies, however, a continuous measurement approach like eddy covariance would be
443 generally more efficient than traditional sampling at regular intervals. Eddy covariance accounts for temporal
444 variability and provides high temporal resolution data by continuously measuring wind speed, gas concentration,
445 and vertical turbulent fluxes to estimate methane emissions (Erkkilä et al., 2018). More importantly, it also offers
446 spatially integrated measurements, averaging emissions over a larger area and therefore accounts for pond spatial
447 heterogeneity. However, it's worth noting that the choice of monitoring approach depends on various factors,
448 including the specific objectives, available resources, and the characteristics of the emission sources. To accurately
449 capture both short-term variability and lake spatial heterogeneity of methane ebullition and diffusion fluxes, the

450 most efficient approach was found to be a combination of continuous measurements with traditional methods
451 including floating chambers, anchored funnels and boundary model calculations (Schubert et al., 2012; Podgrajsek
452 et al., 2014; Erkkilä et al., 2018). This integrated approach would provide a comprehensive understanding of
453 methane emissions, enabling better estimation and more effective mitigation efforts.

454 **5 Conclusions**

455 Many fishponds are hundreds of years old (Potužák et al., 2007), and as such, they are an integral part of our
456 cultural heritage. Nowadays, ponds face a variety of conflicting interests often leading to a focus on maximising
457 fish production that comes at the expense of other ecological services. Intensification of fish production has
458 brought a transition from the traditional management based on natural processes to practices involving
459 supplementary feeding, fertilisation, and overstocking (Pechar, 2000). These changes coupled with the impacts of
460 climate change has resulted to frequent anoxic events and cyanobacterial blooms that reduce biodiversity and limit
461 recreational activities increasingly valued by the public. Our study not only illustrates common water quality
462 problems in fishponds but also provides compelling evidence that methane emissions in these degraded ecosystems
463 further exacerbates negative climate feedbacks and should be considered in discussions to advance the
464 development of sustainable management.

465 Deciphering the mechanisms that drive spatial and temporal heterogeneity in aquatic ecosystem structure and
466 function not only expands our understanding of pond ecology but also provides insights to improve the
467 management of these ecosystems and the services they provide. Our results suggest that spatial heterogeneity needs
468 to be considered when designing experiments and monitoring programs. Without the spatially resolved sampling,
469 we introduce bias into our datasets, hampering our limnological understanding of the ecosystem's functioning and
470 impeding our ability to accurately estimate rates such as methane emissions on a global scale (DeI Sontro et al.,
471 2018a). In agreement with Kosten et al. (2020), we demonstrated that neglecting ebullition leads to a considerable
472 underestimating of the total CH₄ fluxes. Since there are thousands of these intensively managed fishponds, we
473 argue for changing the management practices toward sustainable use of natural resources to mitigate the overall
474 emissions of greenhouse gases from these ecosystems. Future studies are needed to characterise CH₄ fluxes over
475 a greater number and diversity of aquaculture ponds and examine the mechanisms controlling CH₄ emissions in
476 aquatic ecosystems.

477 **Data availability**

478 Dataset associated with the manuscript can be found in the GitHub Repositories under
479 <https://zenodo.org/badge/latestdoi/587640213>.

480 **Author contributions**

481 All authors contributed to the study conception and design. PZ planned the campaign; PZ, AM and JN performed
482 the sampling and analyzed the data; AM performed the gas-measurements; VK performed statistical analyses and
483 modelling; PZ and AM wrote the manuscript. All authors read and approved the final manuscript.

484 **Competing interests**

485 The authors declare that they have no conflict of interest.
486

487 **Acknowledgements**

488 The study was supported by the Czech Science Foundation (Research Projects No. 17-09310S, 19-23261S and
489 P504/19-16554S). We thank Martin Rulík for providing us gas chambers. We especially thank to Miloslav Šimek
490 and Linda Jiřová for enabling gas analyses. We are grateful Anna Sieczko for consultation on the calculation of
491 CH₄ fluxes. English correction was made by Anton Baer.
492

493 **References**

494 Aben, R.C.H., Barros, N., van Donk, E., Frenken, T., Hilt, S., Kazanjian, G., Lamers, L.P.M., Peeters, E.T.H.M.,
495 Roelofs, J.G. M, de Senerpont Domis, L.N., Stephan, S., Velthuis, M., Van de Waal, D.B., Wik, M., Thornton,
496 B.F., Wilkinson, J., DelSontro, T., and Kosten, S.: Cross continental increase in methane ebullition under climate
497 change. *Nat. Commun.*, 8, 1682, <https://doi.org/10.1038/s41467-017-01535-y>, 2017.
498 Banerjee, A., Chakrabarty, M., Rakshit, N., Bhowmick, A.R., and Ray, S.: Environmental factors as indicators of
499 dissolved oxygen concentration and zooplankton abundance: deep learning versus traditional regression approach.
500 *Ecol. Indic.*, 100, 99-117, <https://doi.org/10.1016/j.ecolind.2018.09.051>, 2019.
501 Baron, A.A.P., Dyck, L.T., Amjad, H., Bragg, J., Kroft, E., Newson, J., Oleson, K., Casson, N.J., North, R.L.,
502 Venkiteswaran, J.J., and Whitfield, C.J.: Differences in ebullitive methane release from small, shallow ponds
503 present challenges for scaling. *Sci. Total Environ.*, 802, 149685, <https://doi.org/10.1016/j.scitotenv.2021.149685>,
504 2022.
505 Bartosiewicz, M., Maranger, R., Przytulska, A., and Laurion, I.: Effects of phytoplankton blooms on fluxes and
506 emissions of greenhouse gases in a eutrophic lake. *Water Res.*, 196, 116985,
507 <https://doi.org/10.1016/j.watres.2021.116985>, 2021.

508 Bastviken, D., Cole, J., Pace M., and Tranvik, L.: Methane emissions from lakes: Dependence of lake
509 characteristics, two regional assessments, and a global estimate. *Global Biogeochem. Cycles*, 18, GB4009,
510 <https://doi.org/10.1029/2004GB002238>, 2004.

511 Bastviken, D., Cole, J.J., Pace, M.L., and Van de Bogert, M.C.: Fates of methane from different lake habitats:
512 connecting whole-lake budgets and CH₄ emissions. *J. Geophys. Res. Biogeosci.*, 113, G02024,
513 <https://doi.org/10.1029/2007JG000608>, 2008.

514 Bastviken, D., Santoro, A.L., Marotta, H., Pinho, L.Q., Calheiros, D.F., Crill, P., and Enrich-Prast, A.: Methane
515 Emissions from Pantanal, South America, during the Low Water Season: Toward More Comprehensive Sampling.
516 *Environ. Sci. Tech.*, 44, 5450-5455, <https://doi.org/10.1021/es1005048>, 2010.

517 Bates, D., Maechler, M., Bolker, B., and Walker, S.: Fitting Linear Mixed-Effects Models Using lme4. *J. Stat.*
518 *Soft.*, 67, 1-48, <https://doi.org/10.18637/jss.v067.i01>, 2015.

519 Baxa, M., Musil, M., Kummel, M., Hazlík, O., Tesařová, B., and Pechar, L.: Dissolved oxygen deficits in a shallow
520 eutrophic aquatic ecosystem (fishpond) – Sediment oxygen demand and water column respiration alternately drive
521 the oxygen regime. *Sci. Total Environ.*, 766, 142647, <https://doi.org/10.1016/j.scitotenv.2020.142647>, 2021.

522 Berberich, M.E., Beaulieu, J.J., Hamilton, T.L., Waldo, S., and Buffam, I.: Spatial variability of sediment methane
523 production and methanogen communities within a eutrophic reservoir: Importance of organic matter source and
524 quantity. *Limnol. Oceanogr.*, 65, 1336-1358, <https://doi.org/10.1002/lno.11392>, 2020.

525 Bižić, M., Klintzsch, T., Ionescu, D., Hindiyeh, M.Y., Günthel, M., Muro-Pastor, A.M., Eckert, W., Ulrich, T.,
526 Keppler, F., and Grossart, H.P.: Aquatic and terrestrial cyanobacteria produce methane. *Sci. Adv.*, 6, 1-10,
527 <https://doi.org/10.1126/sciadv.aax5343>, 2020.

528 Bussmann, I., Matoušů, A., Osudar, R., and Mau, S.: Assessment of the radio ³H-CH₄ tracer technique to measure
529 aerobic methane oxidation in the water column. *Limnol. Oceanogr.- Meth.*, 13, 312-327,
530 <https://doi.org/10.1002/lom3.10027>, 2015.

531 Casper, P., Maberly, S.C., Hall, G.H., and Finlay, B.J.: Fluxes of methane and carbon dioxide from a small
532 productive lake to the atmosphere. *Biogeochemistry*, 49, 1-19, <https://doi.org/10.1023/A:1006269900174>, 2000.

533 Čech, M., Peterka, J., Říha, M., Muška, M., Hejzlar, J., and Kubečka, J.: Location and timing of the deposition of
534 eggs strands by perch (*Perca fluviatilis* L.): the roles of lake hydrology, spawning substrate and female size.
535 *Knowl. Manag. Aquat. Ecosyst.*, 403, 1-12, <https://doi.org/10.1051/kmae/2011070>, 2011.

536 Céréghino, R., Biggs, J., Oertli, B., and Declerck, S.: The ecology of European ponds: defining the characteristics
537 of a neglected freshwater habitat. *Hydrobiologia*, 597, 1-6, <https://doi.org/10.1007/s10750-007-9225-8>, 2008.

538 Coumou, D. and Rahmstorf, S.: A decade of weather extreme. *Nat. Clim. Change*, 2, 491-96,
539 <https://doi.org/10.1038/nclimate1452>, 2012.

540 Crusius, J. and Wanninkhof, R.: Gas transfer velocities measured at low wind speed over a lake. *Limnol. Oceanogr.*,
541 48, 1010-1017, <https://doi.org/10.4319/lo.2003.48.3.1010>, 2003.

542 Czikowsky, M.J., MacIntyre, S., Tedford, E.W., Vidal, J., and Miller, S.D.: Effects of wind and buoyancy on
543 carbon dioxide distribution and air-water flux of a stratified temperate lake. *J. Geophys. Res. Biogeosci.*, 123,
544 2305-2322, <https://doi.org/10.1029/2017JG004209>, 2018.

545 De Meester, L., Declerck, S., Stoks, R., Louette, G., Van de Meutter, F., De Bie, T., Michels, E., and Brendonck,
546 L.: Ponds and pools as model systems in conservation biology, ecology and evolutionary biology. *Aquat. Cons.*,
547 15, 715-725, <https://doi.org/10.1002/aqc.748>, 2005.

548 DelSontro, T., Boutet, L., St-Pierre, A., del Giorgio, P.A., and Prairie, Y.T.: Methane ebullition and diffusion from
549 northern ponds and lakes regulated by the interaction between temperature and system productivity. *Limnol.*
550 *Oceanogr.*, 61, 62-77, <https://doi.org/10.1002/lno.10335>, 2016.

551 DelSontro, T., Beaulieu, J.J., and Downing, J.J.: Greenhouse gas emissions from lakes and impoundments:
552 upscaling in the face of global change. *Limnol. Oceanogr. Lett.*, 3, 64-75, <https://doi.org/10.1002/lol2.10073>,
553 2018a.

554 DelSontro, T., del Giorgio, P.A., and Prairie, Y.T.: No Longer a Paradox: The Interaction Between Physical
555 Transport and Biological Processes Explains the Spatial Distribution of Surface Water Methane Within and Across
556 Lakes. *Ecosystems*, 21, 1073-1087, [10.1007/s10021-017-0205-1](https://doi.org/10.1007/s10021-017-0205-1), 2018b.

557 Emerson, J.B., Varner, R.K., Wik, M., Parks, D.H., Neumann, R.B., Johnson, J.E., Singleton, C. M., Woodcroft,
558 B.J., Tollerson II, R., Owusu-Domney, A., Binder, M., Freitas, N. L., Crill, P.M., Saleska, S.R., Tyson, G.W., and
559 Rich, V.I.: Diverse sediment microbiota shape methane emission temperature sensitivity in Arctic lakes. *Nat.*
560 *Commun.*, 12, 5815, <https://doi.org/10.1038/s41467-021-25983-9>, 2021.

561 Erkkilä, K.-M., Ojala, A., Bastviken, D., Biermann, T., Heiskanen, J. J., Lindroth, A., Peltola, O., Rantakari, M.,
562 Vesala, T., and Mammarella, I.: Methane and carbon dioxide fluxes over a lake: comparison between eddy
563 covariance, floating chambers and boundary layer method, *Biogeosciences*, 15, 429–445,
564 <https://doi.org/10.5194/bg-15-429-2018>, 2018.

565 Grasset, Ch., Mendonça, R., Saucedo, G.V., Bastviken, D., Roland, F., and Sobek, S.: Large but variable methane
566 production in anoxic freshwater sediment upon addition of allochthonous and autochthonous organic matter.
567 *Limnol. Oceanogr.*, 63, 1488-1501, <https://doi.org/10.1002/lno.10786>, 2018.

568 Halekoh, H. and Hojsgaard, S.: A Kenward-Roger Approximation and Parametric Bootstrap Methods for Tests in
569 Linear Mixed Models - The R Package pbrtest. *J. Stat. Soft.*, 59, 1-30, <https://doi.org/10.18637/jss.v059.i09> 2014.

570 Hofmann, H., Federwisch, L., and Peeters, F.: Wave-induced release of methane: littoral zones as a source of
571 methane in lakes. *Limnol. Oceanogr.*, 55, 1990-2000, <https://doi.org/10.4319/lo.2010.55.5.1990>, 2010.

572 Hofmann, H.: Spatiotemporal distribution patterns of dissolved methane in lakes: How accurate are the current
573 estimations of the diffusive flux path? *Geophys. Res. Lett.*, 40, 2779-2784, <https://doi.org/10.1002/grl.50453>,
574 2013.

575 Hu, Z., Wu, S., Ji, Ch., Zou, J., Zhou, Q., and Liu, S.: A comparison of methane emissions following rice paddies
576 conversion to crab-fish farming wetlands in southeast China. *Environ. Sci. Pollut. Res.*, 23, 1505-1515,
577 <https://doi.org/10.1007/s11356-015-5383-9>, 2016.

578 Jansen, J., Thornton, B.F., Jammot, M.M., Wik, M., Cortés, A., Friborg, T., MacIntyre, S., and Crill, P.M.:
579 Climate-sensitive controls on large spring emissions of CH₄ and CO₂ from northern lakes. *J. Geophys. Res.*,
580 *Biogeosciences*, 124, 2379-2399, <https://doi.org/10.1029/2019JG005094>, 2019.

581 Jähne, B., Münnich, K. O., Bösinger, R., Dutzi, A., Huber, W., and Libner, P.: On the parameters influencing air-
582 water gas exchange, *J. Geophys. Res.*, 92, C2, 1937-1949, [doi:10.1029/JC092iC02p01937](https://doi.org/10.1029/JC092iC02p01937), 1987.

583 Jeppesen, E., Søndergaard, M., Sortkjaer, O., Mortensen, E., and Kristensen, P.: Interactions between
584 phytoplankton zooplankton and fish in a shallow hypertrophic Lake a study of phytoplankton collapses in Lake
585 Sobygaard, Denmark. *Hydrobiologia*, 1991, 149-164, <https://doi.org/10.1007/BF00026049>, 1990.

586 Kolar, V., Vlašánek, P., and Boukal, D.S.: The influence of successional stage on local odonate communities in
587 man-made standing waters. *Ecol. Eng.*, 173, 106440, <https://doi.org/10.1016/j.ecoleng.2021.106440>, 2021.

588 Kopáček, J. and Hejzlar, J.: Semi-micro determination of total phosphorus in fresh waters with perchloric acid
589 digestion. *Int. J. Environ. Anal. Chem.*, 53, 173-183, <https://doi.org/10.1080/03067319308045987>, 1993.

590 Kopáček, J. and Procházková, L.: Semi-Micro Determination of Ammonia in Water by the Rubazotic Acid Method.
591 *Int. J. Environ. Anal. Chem.*, 53, 243-248, <https://doi.org/10.1080/03067319308045993>, 1993.

592 Kosten, S., Almeida, R.M., Barbosa, I., Mendonça, R., Muzitano, I.S., Oliveira-Junior, E.S., Vroom, R.J.E., Wang,
593 H.J., and Barros, N.: Better assessments of greenhouse gas emissions from global fish ponds needed to adequately
594 evaluate aquaculture footprint. *Sci. Total Environ.*, 748, 141247, <https://doi.org/10.1016/j.scitotenv.2020.141247>,
595 2020.

596 Laas, A., Noges, P., Koiv, T., and Noges, T.: High-frequency metabolism study in a large and shallow temperate
597 lake reveals seasonal switching between net autotrophy and net heterotrophy. *Hydrobiologia*, 694, 57-74,
598 <https://doi.org/10.1007/s10750-012-1131-z>, 2012.

599 Loken, L.C., Crawford, J.T., Schramm, P.J., Stadler, P., Desai, A.R., and Stanley, E.H.: Large spatial and temporal
600 variability of carbon dioxide and methane in a eutrophic lake. *J. Geophys. Res. Biogeosci.*, 124, 2248-2266
601 <https://doi.org/10.1029/2019JG005186>, 2019.

602 Lüdecke, D.: “ggeffects: Tidy Data Frames of Marginal Effects from Regression Models.” *J. Open Source Soft.*,
603 3, 772, <https://doi.org/10.21105/joss.00772>, 2018.

604 Lüdecke, D., Makowski, D., and Waggoner, P.: performance: Assessment of Regression Models Performance. R
605 package version 0.4.4. <https://CRAN.R-project.org/package=performance>, 2020.

606 Ma, Y., Sun, L., Liu, C., Yang, X., Zhou, W., Yang, B., Schwenke, G., and Liu, D.L.: A comparison of methane
607 and nitrous oxide emissions from inland mixed-fish and crab aquaculture ponds. *Sci. Total Environ.*, 637-638,
608 517-523, <https://doi.org/10.1016/j.scitotenv.2018.05.040>, 2018

609 McAuliffe, C.: Gas Chromatographic determination of solutes by multiple phase equilibrium. *Chem. Technol.*, 1,
610 46-51, 1971.

611 Miranda, L.E., Hargreaves, J.A., and Raborn, S.W.: Predicting and managing risk of unsuitable dissolved oxygen
612 in a eutrophic lake. *Hydrobiologia*, 457, 177-185, <https://doi.org/10.1023/A:1012283603339>, 2001.

613 Murphy, J. and Riley, J.P.: A modified single-solution method for the determination of phosphate in natural waters.
614 *Anal. Chim. Acta*, 27, 31-36, [https://doi.org/10.1016/S0003-2670\(00\)88444-5](https://doi.org/10.1016/S0003-2670(00)88444-5), 1962.

615 Natchimuthu, S., Sundgren, I., Gålfalk, M., Klemetsson, L., Crill, P., Danielsson, Å., and Bastviken, D.: Spatio-
616 temporal variability of lake CH₄ fluxes and its influence on annual whole lake emission estimates. *Limnol.*
617 *Oceanogr.*, 61, 13-26, <https://doi.org/10.1002/lno.10222>, 2016.

618 Nijman, T.P.A., Lemmens, M., Lurling, M., Kosten, S., Welte, C., and Veraart, A.J.: Phosphorus control and
619 dredging decrease methane emissions from shallow lakes. *Sci. Total Environ.*, 847, 15758,
620 <https://doi.org/10.1016/j.scitotenv.2022.157584>, 2022.

621 Ortiz, D.A. and Wilkinson, G.M.: Capturing the spatial variability of algal bloom development in a shallow
622 temperate lake. *Freshwater Biol.*, 66, 2064-2075, <https://doi.org/10.1111/fwb.13814>, 2021.

623 Pechar, L.: Impacts of long-term changes in fishery management on the trophic level and water quality in Czech
624 fishponds. *Fisheries Manag. Ecol.*, 7, 23-32, [10.1046/j.1365-2400.2000.00193.x](https://doi.org/10.1046/j.1365-2400.2000.00193.x), 2000.

625 Pokorný, J. and Hauser, V.: The restoration of fish ponds in agricultural landscapes. *Ecol. Eng.*, 18, 555-574,
626 [https://doi.org/10.1016/S0925-8574\(02\)00020-4](https://doi.org/10.1016/S0925-8574(02)00020-4), 2002.

627 Podgrajsek, E., Sahlée, E., Bastviken, D., Holst, J., Lindroth, A., Tranvik, L., and Rutgersson, A.: Comparison of
628 floating chamber and eddy covariance measurements of lake greenhouse gas fluxes, *Biogeosciences*, 11, 4225–
629 4233, <https://doi.org/10.5194/bg-11-4225-2014>, 2014.

630 Potužák, J., Hůda, J., and Pechar, L.: Changes in fish production effectivity in eutrophic fishponds – impact of
631 zooplankton structure. *Aquacult. Int.*, 15, 201-210, <https://doi.org/10.1007/s10499-007-9085-2>, 2007.

632 Potužák, J., Duras, J., and Drozd, B.: Mass balance of fishponds: are they sources or sinks of phosphorus?
633 *Aquacult. Int.*, 24, 1725-1745, <https://doi.org/10.1007/s10499-016-0071-4>, 2016.

634 Prairie, Y.T. and del Giorgio, P.A.: A new pathway of freshwater methane emissions and the putative importance
635 of microbubbles. *Inland Waters*, 3, 311-320, <https://doi.org/10.5268/IW-3.3.542>, 2013.

636 Procházková, L.: Bestimmung der Nitrate im Wasser. *Zeitschrift für Analytische Chemie*, 167, 254-260, 1959.

637 Rasilo, T., Prairie, Y.T., and del Giorgio, P.A.: Large-scale patterns in summer diffusive CH₄ fluxes across boreal
638 lakes, and contribution to diffusive C emissions. *Glob. Change Biol.*, 21, 1124-1139,
639 <https://doi.org/10.1111/gcb.12741>, 2015.

640 R Core Team: A language and environment for statistical computing. R Foundation for Statistical Computing,
641 Vienna, Austria <https://www.R-project.org/>, 2018.

642 Reynolds, C.S.: *Ecology of phytoplankton*, Cambridge University Press, Cambridge,
643 <https://doi.org/10.1017/CBO9780511542145>, 2006.

644 Rinke, K., Huber, A.M.R., Kempke, S., Eder, M., Wolf, T., Probst, W.N., and Rothhaupt, K.: Lake-wide
645 distributions of temperature, phytoplankton, zooplankton, and fish in the pelagic zone of a large lake. *Limnol.*
646 *Oceanogr.*, 54, 1306-1322, <https://doi.org/10.4319/lo.2009.54.4.1306>, 2009.

647 Rutegwa, M., Potužák, J., Hejzlar, J., and Drozd, B.: Carbon metabolism and nutrient balance in a hypereutrophic
648 semi-intensive fishpond. *Knowl.Manag. Aquat. Ecosyst.*, 49, <https://doi.org/10.1051/kmae/2019043>, 2019.

649 Sanseverino, A.M., Bastviken, D., Sundh, I., Pickova, J., and Enrich-Prast, A.: Methane carbon supports aquatic
650 food webs to the fish level. *PLoS One* 7, e42723, <https://doi.org/10.1371/journal.pone.0042723>, 2012.

651 Scheffer, M.: *Ecology of shallow lakes*. Population and Community Biology Series. Springer, 357 p.,
652 <https://doi.org/10.1007/978-1-4020-3154-0>, 2004.

653 Schilder, J., Bastviken, D., van Hardenbroek, M., Kankaala, P., Rinta, P., Stötter, T., and Heiri, O.: Spatial
654 heterogeneity and lake morphology affect diffusive greenhouse gas emission estimates of lakes. *Geophys. Res.*
655 *Lett.*, 40, 5752-5756, <https://doi.org/10.1002/2013GL057669>, 2013.

656 Schmiedeskamp, M., Praetzel, L.S.E., Bastviken, D., and Knorr, K.H.: Whole-lake methane emissions from two
657 temperate shallow lakes with fluctuating water levels: Relevance of spatiotemporal patterns. *Limnol. Oceanogr.*,
658 66, 2455-2469, <https://doi.org/10.1002/lno.11764>, 2021.

659 Schubert, C.J., Diem, T., Eugster W.: Methane emissions from a small wind shielded lake determined by eddy
660 covariance, flux chambers, anchored funnels, and boundary model calculations: a comparison. *Environ. Sci.*
661 *Technol.*, 46, 4515-4522, <https://doi.org/10.1021/es203465x>, 2012

662 Stanley, E.H., Collins, S.M., Lottig, N.R., Oliver, S.K., Webster, K.E., Cheruvilil, K.S., and Soranno, P.A.: Biases
663 in lake water quality sampling and implications for macroscale research. *Limnol. Oceanogr.*, 64, 1572-1585,
664 <https://doi.org/10.1002/lno.11136>, 2019.

665 Stockwell, J.D., Doubek, J.P., Adrian, R., Anneville, O., Carey, C.C., Carvalho, L., Domis, L.N.D.S., Dur, G.,
666 Frassl, M.A., Grossart, H.-P., Ibelings, B.W., Lajeunesse, M.J., Lewandowska, A.M., Llames, M.E., Matsuzaki,

667 S.-I.S., Nodine, E.R., Nöges, P., Patil, V.P., Pomati, F., Rinke, K., Rudstam, L.G., Rusak, J.A., Salmaso, N.,
668 Seltmann, C.T., Straile, D., Thackeray, S.J., Thiery, W., Urrutia-Cordero, P., Venail, P., Verburg, P., Woolway,
669 R.I., Zohary, T., Andersen, M.R., Bhattacharya, R., Hejzlar, J., Janatian, N., Kpodonu, A.T.N.K., Williamson,
670 T.J., and Wilson, H.L.: Storm impacts on phytoplankton community dynamics in lakes. *Glob. Change Biol.*, 26,
671 2756-2784, <https://doi.org/10.1111/gcb.15033>, 2020.

672 van Bergen, T.J.H.M., Barros, N., Mendonça, R., Aben, R.C.H., Althuisen, I.H.J., Huszar, V., Lamers, L.P.M.,
673 Lüring, M., Roland, F., Kosten, S.: Seasonal and diel variation in greenhouse gas emissions from an urban pond
674 and its major drivers. *Limnol. Oceanogr.*, 64, 2129-2139, <https://doi.org/10.1002/lno.11173>, 2019.

675 Varadharajan, Ch. and Hemond, H.F.: Time-series analysis of high-resolution ebullition fluxes from a stratified,
676 freshwater lake. *J. Geophys. Res.*, 117, G02004, <https://doi.org/10.1029/2011JG001866>, 2012.

677 Wanninkhof, R.: Relationship between wind speed and gas exchange over the ocean revisited. *Limnol. Oceanogr.*
678 *Methods*, 12, 351-362, <https://doi.org/10.4319/lom.2014.12.351>, 2014.

679 Wiesenburg, D.A. and Guinasso N.L.: Equilibrium solubilities of methane, carbon monoxide, and hydrogen in
680 water and sea water. *J. Chem. Eng. Data*, 24, 356-360, <https://doi.org/10.1021/je60083a006>, 1979.

681 Wik, M., Varner, R.K., Anthony, K.W., MacIntyre, S., and Bastviken, D.: Climate-sensitive northern lakes and
682 ponds are critical components of methane release. *Nat. Geosci.*, 9, 99-105, <https://doi.org/10.1038/ngeo2578>,
683 2016.

684 Xiao, Q., Zhang, M., Hu, Z., Gao, Y., Hu, Ch., Liu, Ch., Liu, S., Zhang, Z., Zhao, J., Xiao, W., and Lee, X.: Spatial
685 variations of methane emission in a large shallow eutrophic lake in subtropical climate. *J. Geophys. Res.*
686 *Biogeosci.*, 122, <https://doi.org/10.1002/2017JG003805>, 2017.

687 Yamamoto, S., Alcauskas, J.B., and Crozier, T.E. Solubility of methane in distilled water and seawater. *J. Chem.*
688 *Eng. Data*, 21, 78-80, <https://doi.org/10.1021/je60068a029>, 1976.

689 Yan, X., Xu, X., Ji, M., Zhang, Z., Wang, M., Wu, S., Wang, G., Zhang, Ch., and Liu, H.: Cyanobacteria blooms:
690 A neglected facilitator of CH₄ production in eutrophic lakes. *Sci. Total Environ.*, 651, 466-474,
691 <https://doi.org/10.1016/j.scitotenv.2018.09.197>, 2019.

692 Yang, P., Zhang, Y., Yang, H., Zhang, Y., Xu, J., Tan, L., Tong, C., and Lai, D.Y.: Large fine-scale spatiotemporal
693 variations of CH₄ diffusive fluxes from shrimp aquaculture ponds affected by organic matter supply and aeration
694 in Southeast China. *J. Geophys. Res. Biogeosci.*, 124, 1290-1307, <https://doi.org/10.1029/2019JG005025>, 2019.

695 Yang, P., Zhang, Y., Yang, H., Guo, Q., Lai, D.Y.F., Zhao, G., Li, L., and Tong, C.: Ebullition was a major
696 pathway of methane emissions from the aquaculture ponds in Southeast China. *Water Res.*, 184, 116176,
697 <https://doi.org/10.1016/j.watres.2020.116176>, 2020.

698 Yuan, J., Xiang, J., Liu, D.Y., Kang, H., He, T.H., Kim, S., Lin, Y.X., Freeman, C., and Ding, W.X.: Rapid growth
699 in greenhouse gas emissions from the adoption of industrial-scale aquaculture. *Nat. Clim. Chang.*, 9, 318-322,
700 <https://doi.org/10.1038/s41558-019-0425-9>, 2019.

701 Yuan, J., Liu, D., Xiang, J., He, T., Kang, H., and Ding, W.: Methane and nitrous oxide have separated production
702 zones and distinct emission pathways in freshwater aquaculture ponds. *Water Research*, 190, 116739,
703 <https://doi.org/10.1016/j.watres.2020.116739>, 2021.

704 Zar, J.H.: *Biostatistical analysis*. Prentice Hall, Inc., Englewood Cliffs, New York, 663 p., 1984.

705 Zhang, L., Liao, Q., Gao, R., Luo, R., Liu, Ch., Zhong, J., and Wang, Z.: Spatial variations in diffusive methane
706 fluxes and the role of eutrophication in a subtropical shallow lake. *Sci. Total Environ.*, 759, 143495,
707 <https://doi.org/10.1016/j.scitotenv.2020.143495>, 2021.

708 Zhao, J., Zhang, M., Xiao, W., Jia, L., Zhang, X., Wang, J., Zhang, Z., Xie, Y., Yini Pu, Liu, S., Feng, Z., Lee X.:
709 Large methane emission from freshwater aquaculture ponds revealed by long-term eddy covariance observation.
710 *Agric. For. Meteorol.*, 308-309, 108600, <https://doi.org/10.1016/j.agrformet.2021.108600>, 2021.

711 Zhou, Y.Q., Zhou, L., Zhang, Y.L., de Souza, J.G., Podgorski, D.C., Spencer, R.G.M., Jeppesen, E., and Davidson,
712 T.A.: Autochthonous dissolved organic matter potentially fuels methane ebullition from experimental lakes. *Water*
713 *Res.*, 166, 115048, <https://doi.org/10.1016/j.watres.2019.115048>, 2019.

714 Zuur, A.F., Ieno, E.N., Walker, N.J., Saveliev, A.A., and Smith, G.M.: *Mixed effects models and extensions in*
715 *ecology with R*. Springer, New York, USA, 574 p, <https://doi.org/10.1007/978-0-387-87458-6>, 2009.